Functional relation between growth, photosynthetic rate and regulation in the coastal picoeukaryote Phaeomonas sp. RCC 503 (Pinguiophyceae, Stramenopiles)

Vasco Giovagnetti, Maria Letizia Cataldo, Fabio Conversano, Christophe Brunet

OXFORD UNIVERSITY PRESS Journal of Plankton Research

Functional relation between growth, photosynthetic rate and regulation in the coastal picoeukaryote Phaeomonas sp. RCC 503 (Pinguiophyceae, Stramenopiles)

Journal:	*Journal of Plankton Research*
Manuscript ID:	JPR-2010-094.R1
Manuscript Type:	Original Article
Date Submitted by the Author:	27-May-2010
Complete List of Authors:	Giovagnetti, Vasco; Stazione Zoologica A. Dorhn, Laboratory of Ecology and Evolution of Plankton Cataldo, Maria Letizia; Stazione Zoologica A. Dorhn, Laboratory of Ecology and Evolution of Plankton Conversano, Fabio; Stazione Zoologica A. Dorhn, Laboratory of Ecology and Evolution of Plankton Brunet, Christophe; Stazione Zoologica A. Dorhn, Laboratory of Ecology and Evolution of Plankton
Keywords:	photoacclimation, picoeukaryote, xanthophyll cycle

Functional relation between growth, photosynthetic rate and regulation in the coastal picoeukaryote *Phaeomonas sp.* RCC 503 (Pinguiophyceae, Stramenopiles)

V. GIOVAGNETTI, M. L. CATALDO, F.CONVERSANO AND C. BRUNET*

Laboratory of Ecology and Evolution of Plankton, Stazione Zoologica Anton Dohrn,Villa Comunale, 80121 Naples, Italy

*: CORRESPONDING AUTHOR: christophe.brunet@szn.it

Running head: *Phaeomonas sp.* RCC 503 photoregulation and growth

Key-words: photoacclimation; picoeukaryote; xanthophyll cycle.

Abbreviations: Ax, antheraxanthin; DPS, de-epoxidation state [DPS = Zx : (Vx + Ax + Zx)]; ETR, electron transport rate; Fv : Fm, PSII maximum photochemical efficiency; LHC, light-harvesting complex; Neox, neoxanthin; NPQ, non-photochemical quenching; PAM, pulse amplitude modulation; PFD, photon flux density; Vx, violaxanthin; Zx, zeaxanthin.

ABSTRACT

Picoeukaryotes constitute good models for testing photophysiological hypotheses because of constrains as well as opportunities related to their minute size. This study was undertaken to investigate the relation between growth rate and regulation of photosynthesis in a coastal picoeukaryote, using the strain *Phaeomonas sp.* RCC 503 as a model. Here we address how photoacclimation responses affect photosynthetic capacity and how growth rate is modulated by photoacclimation and photosynthetic rate variations. Growth of the strain was followed over five days under five sinusoidal light regimes set to peak at maximal photon flux densities (PFD) of 10, 50, 100, 250 and 500 µmol photons m^{-2} s^{-1}. We measured growth rate, pigment composition, variable fluorescence, non-photochemical quenching, electron transport rate, absorption spectrum, cell carbon and nitrogen content one to three times per day under each of these five conditions. Results suggest that *Phaeomonas sp.* RCC 503 is a light-adapted species, showing a high physiological plasticity allowing it to grow under a broad range of PFD conditions. The PFD determined growth rate, the latter being correlated significantly to photosynthetic capacity. Biochemical properties of cells, in term of carbon and nitrogen content were closely correlated to growth rate and PFD. Photoacclimation allows growth to be maintained at low irradiance except at 10 µmol photons m^{-2} s^{-1}, whereas photoprotection efficiency allows enhancement of growth at high PFDs.

INTRODUCTION

In the field, maximum light intensity available for photosynthesis varies predictably over daily and annual cycles. Yet, superimposed on these cycles are such factors as cloud cover that affect the amount of incoming light in an unpredictable way. For phytoplankton, and especially coastal phytoplankton, mild turbulence of the water column adds even further to this unpredictability (Lewis *et al*., 1984; MacIntyre *et al*., 2000; Lichtman and Klausmeier, 2001); one moment a cell finds itself at depth where its photosystems must cope with low light intensity, whereas the next moment it may be transported up to the surface where its photosystems have to adjust itself rapidly to conditions approaching full sunlight.

Phytoplankton cells possess a number of physiological acclimation and regulatory responses to cope with these unpredictable, potentially extreme, and often rapid changes in light intensity (MacIntyre *et al*., 2002; Raven and Geider, 2003).

Acclimation involves net synthesis or breakdown of macromolecules and so changes in pigment quota, stoichiometry of cell components, and ultrastructural changes in the cell. Regulation refers to faster processes than acclimatory ones (i.e. time constants of seconds to minutes) acting through the control of enzyme activities and energy dissipation pathways (Raven and Geider, 2003). Regulatory processes therefore allow photosynthesis to react instantaneously and reversibly the environmental changes occurring. These mechanisms include the Rubisco activity, state transition mechanism, and the xanthophyll cycle (Raven and Geider, 2003). The xanthophyll cycle (XC) is one of the main processes involved in the dissipation of excessively absorbed light energy through the non-photochemical quenching (NPQ, Finazzi *et al*., 2006). In green algae and higher plants, and in other algal groups (i.e. Pinguiophyceae), the XC mechanism is based on the reversible de-epoxidation of violaxanthin (Vx) into zeaxanthin (Zx) through antheraxanthin (Ax). In most chlorophyll *c* (Chl *c*) containing phytoplankton species (e.g. Diatoms), it involves the inter-conversion between diadinoxanthin (Dd) and diatoxanthin (Dt; Stransky and Hager, 1970; Lavaud *et al*., 2007; Dimier *et al*., 2007 b). Accumulation of Zx or Dt is triggered by the formation of a pH gradient across the thylakoid membrane (e.g., see the review by Goss and Jakob, *in press*).

Little is known about the picoeukaryotes with respect to their ecophysiological features (Timmermans *et al*., 2005; Dimier *et al*., 2007 a, 2009; Six *et al*., 2008, 2009). These small planktonic photolithotrophs usually dominate oligotrophic water ecosystems, reaching up to almost 50 percent of total biomass and production, while in eutrophic waters their contribution to the phytoplankton community is lower (Not *et al*., 2005; Worden and Not, 2008). Their small size explains many of their biological and ecological features such as the large surface area per unit volume and the minimal diffusion boundary layer (i.e. higher nutrient consumption rates), the low sinking rate, the low packaging effect and the efficient light utilization (Raven, 1998; Raven *et al*., 2005).

High plasticity in photosynthetic regulation has been described in picoeukaryotes. For instance, Six and collaborators (Six *et al*., 2008, 2009) highlighted different photoacclimation strategies in three ecotypes of *Ostreococcus* related to their ecological niches. Intraspecific variability has been shown in *Pelagomomans calceolata* (Dimier *et al*., 2009 a), demonstrating different photosynthetic regulation strategies in response to irradiance dynamics.

All these properties make picoeukaryotes interesting models for physiological studies aiming to analyze the functional responses of algae to environmental changes, and for instance to photon flux density (PFD) variability. The purpose of our experimentation was to investigate the relation between growth rate, photosynthetic capacity and photoacclimative process efficiency in the coastal picoeukaryote *Phaeomonas sp.* (strain RCC503, Pinguiophyceae, Stramenopiles). Physiological response curve (PRC, Peek *et al*., 2002) experiments were performed plotting physiological variables and growth rate against a range of PFD. The questions behind this work were: what kind of photoresponses are developed by this species when low and high light conditions are experienced? How do these responses explain photosynthetic efficiency changes?

Population growth was investigated over five days under five different sinusoidal light regimes set to peak at maximal photon flux densities of 10, 50, 100, 250 and 500 µmol photons m^{-2} s^{-1}. Pigments, variable fluorescence, NPQ, electron transport rate, absorption spectra, cell carbon and nitrogen content together with size, volume and cell concentrations were measured one to three times per day during the exponential phase.

METHOD

Algal model and culture conditions

The strain RCC503 of *Phaeomonas sp.* (Pinguiophyceae) was isolated along the Mediterranean Spanish coast and was provided by the Roscoff Culture Collection (Vaulot *et al.*, 2004). The strain was cultivated nonaxenically at 20 °C at 100 µmol photons m^{-2} s^{-1} with a 11:13 hours light : dark photoperiod in locally obtained, and sterilized seawater amended with f/2 medium (Guillard and Ryther, 1962) using 225 cm^2 polystyrene canted-neck flasks (Corning Incorporated, NY, 14831, USA). Cultures were continuously aerated and maintained in exponential phase by daily and semi-continuous dilution (50% of the total volume) over a period of more than two weeks before the experiments. Before performing experiments, we checked pre-acclimation of the strain to the light condition, by assessing stability of pigment content and growth rate.

Experimental design and sampling strategy

After 15 days acclimation period at 100 µmol photons m^{-2} s^{-1}, cultures were subjected to 5 different sinusoidal light (SL, Fig. 1a) regimes, each with a different maximal photon flux density (PFD) of 10 (LL1), 50 (LL2), 100 (ML), 250 (HL1), 500 (HL2) µmol photons m^{-2} s^{-1}, respectively. The mean PFD over the 11 h of illumination ranged between 344 and 7 µmol photons m^{-2} s^{-1}, which is likely similar to the light experienced by cells at a depth of 10 m and at the Deep-Chlorophyll maximum layer in a Mediterranean water column, respectively (see Dimier *et al.*, 2009 a).

Population growth was followed over five days while photophysiological and biochemical properties of *Phaeomonas sp.* were measured during the exponential growth phase. Under the LL conditions, where no exponential phase was observed, sampling of photophysiological and biochemical parameters lasted five days.

Each experiment was performed in triplicate. Flasks were illuminated by the light-bulb kit ACLS (Advanced Control Lighting System) and Infinity XR4 (Aquarium Technologies - Sfiligoi S.r.l., Bassano del Grappa, Italy), simulating light-dark sinusoidal cycles, reproducing dawn and sunset. XR4 is equipped with metallic iodur HQI bulbs

(10000° K). PFD was measured with a 4π quantameter (sensor QSL 2101, Biospherical Instruments Inc., San Diego, CA, USA).

Cultures were sampled three times per day (Fig. 1a). First sampling was carried out during dawn (for HL2 condition, incident irradiance was below 40 µmol photons m^{-2} s^{-1}), while the second corresponded with the irradiance peak. The third one was carried out during sunset (HL2 incident irradiance was below 40 µmol photons m^{-2} s^{-1}). Twenty to fifty milliliters of culture were rapidly taken with a 50 mL syringe during each sampling time, for measuring variable fluorescence, NPQ, electron transport rate, and for further analysis of pigments, absorption spectrum, cell size and volume (by Coulter Counter analysis) and cell concentrations (by microscopic counts).

Temperature and pH were controlled daily with a HI-9214-Stick pH meter (Hanna Instruments, Woonsocket, RI, USA). The growth rate was estimated daily from cell abundance measurements using the following equation:

$$\mu = \ln [N_{t2} : N_{t1}] : [t_2 - t_1] \quad (1)$$

where μ is the growth rate (d^{-1}) and N_t is the mean cell concentration at time t, where t_1 and t_2 correspond to the morning sampling time of days 1 and 2, respectively. From the growth rate, the number of cell divisions (n) per day was estimated with the following equation:

$$n = \mu : [\ln(2)] \quad (2)$$

where n is the number of cell divisions per day and μ is the growth rate.

Pigment analysis

One aliquot of algal culture (10 mL) was filtered onto GF/F glass-fiber filters (Whatman) and immediately stored in liquid nitrogen until analysis. Triplicate samples were taken during each sampling time. Analysis was carried out following the procedure described in Dimier *et al.* (2007 a). The pigment extract was injected in a Hewlett Packard series 1100 HPLC (Hewlett-Packard) with a C8 BDS 3 mm Hypersil, IP column (Thermo Electron).

The mobile phase was composed of two solvent mixtures: methanol and aqueous ammonium acetate (70:30) and methanol. Pigments were detected spectrophotometrically at 440 nm using a Model DAD, Series 1100 Hewlett Packard photodiode array detector. Fluorescent pigments were detected in a Hewlett Packard standard FLD cell series 1100 with excitation and emission wavelengths set at 407 and 665 nm, respectively. Determination and quantification of pigments used pigment standards from D.H.I. Water & Environment (Hørsholm,Denmark).

Variable fluorescence and NPQ

Only during the irradiance peak sampling time wer samples for PAM measurements taken. Photochemical efficiency of PSII was estimated by a Phyto-PAM fluorometer (Heinz Walz GmbH, Effeltrich, Germany). Triplicate measurements of variable fluorescence were performed on both light- and 15-min dark- acclimated samples. The maximum photochemical efficiency (Fv : Fm, with Fv = Fm – Fo) was measured on 15-min dark-acclimated sample during the irradiance peak sampling time. Fm and Fm′ were measured after a saturating pulse of red light (2400 µmol photons m^{-2} s^{-1} for 450 ms) causing a complete reduction of the PSII acceptor pool.

The non-photochemical quenching of fluorescence was quantified by the Stern-Volmer expression:

$$NPQ = (Fm : Fm') - 1 \quad (3)$$

Electron transport rate (ETR) *vs.* light curves were determined on 15-min dark-exposed samples applying ten increasing irradiances (I from 1 to 1500 µmol photons m^{-2} s^{-1}, for 2 min each). The absolute Electron Transport Rate (expressed in e^- Chl a^{-1} h^{-1}) was calculated as follows:

$$_{abs}ETR = (Fv' : Fm') \cdot I \cdot (a^*_{ph} : 2) \quad (4)$$

where I is the incident irradiance (in µmol photons m^{-2} s^{-1}). The mean absorption value (a^*_{ph}) of phytoplankton was normalized by Chl *a* (m^2 mg Chl a^{-1}) and divided by 2 assuming that half of the absorbed light was distributed to PSII.

The ETR-light curves were fitted with the equation of Eilers and Peeters (1988) to estimate the photosynthetic parameters α^B, Ek, $_{abs}ETR_{max}$. The relative Electron Transport Rate ($_{rel}ETR_{max}$) was estimated with equation (4) without Chl *a* normalization.

Organic Carbon and Nitrogen

Samples for the determination of particulate organic carbon (POC) and particulate organic nitrogen (PON) were filtered on pre-combusted (450°C, 5h) glass fiber filters (Whatman GF/F) and immediately stored at - 20 °C. The analyses were performed with a FlashEA 1112 Series Thermo Electron CHN elemental analyzer (Hedges and Stern, 1984). Cyclohexanone-2,4-dinitrophenyl hydrazone was used as standard.

Absorption spectrum

Ten milliliter sample were filtered onto Whatman GF/F filters and immediately frozen. Measurements were carried out following the procedure described in Dimier *et al*. (2007 a). Absorption was measured between 280 nm and 800 nm with 1-nm increments on a spectrophotometer (Hewlett Packard HP-8453E) equipped with an integrating sphere (Labsphere RSA-HP-53). The mean absorption value (a*) was thus normalized by the Chl *a* concentration of the sample to obtain the Chl *a* specific absorption coefficient (a^*_{ph}, m^2 mg Chl a^{-1}).

RESULTS

Growth

Phaeomonas sp. was able to grow under the entire range of light conditions with the exception of LL1 (10 µmol photons m^{-2} s^{-1}) and showed the highest growth rate under the highest light regime (Fig. 1b). At the end of the exponential phase for the HL and ML conditions or at day 5 for LL conditions, where no exponential phase was found, cell concentrations ranged between $1.77 \times 10^4 \pm 1.98 \times 10^3$ and $3.66 \times 10^5 \pm 9.15 \times 10^4$ cells

mL^{-1} following a positive light gradient. Number of divisions per day ranged between 0 and 0.44 d^{-1}. Cell size and volume were 3.27 ± 0.07 µm and 18.65 ± 0.95 µm^3, respectively. Only under the lowest PFD, did cells show a decrease of size and volume (2.86 ± 0.02 µm and 12.28 ± 0.19 µm^3).

Photosynthetic pigments

Together with Chl *a*, many accessory pigments were present in the LHCs of *Phaeomonas sp.* and the main ones were the following: chlorophyll (Chl) c_2, fucoxanthin (Fuco), cis-fucoxanthin (*cis*-Fuco), neoxanthin (Neox), Chl c_3 and ß-carotene (ß-Car).

The mean Chl *a* content per cell was significantly higher in LL conditions compared to the ML or HL ones ranging between $9.96 \times 10^{-17} \pm 1.93 \times 10^{-17}$ and $2.82 \times 10^{-16} \pm 7.13 \times 10^{-17}$ mol Chl *a* cell^{-1} (Fig. 2a). It can be seen that a higher Chl *a* cell^{-1} value was measured under HL2 relative to HL1.

Lowering of the light harvesting capacity under high light was revealed by the decrease of almost all main accessory pigments (Fig. 2b, c), in agreement with the lower Chl *a* specific absorption coefficient (a^*_{ph}, data not shown). Following their distribution over the different PFD gradient, three groups of accessory pigments could be defined. The first group was formed by Chl c_2 and fucoxanthin (Fig. 2b and c, respectively) as well as violaxanthin and antheraxanthin (see xanthophyll cycle paragraph) showing similar values at LL1 and LL2. Minor pigments such as Chl c_3, cis-fucoxanthin and ß-carotene (Fig. 2b and c, respectively) belonged to the second group characterized by an increase from LL2 to LL1, as the Chl *a* pool. Pigments of the third group (neoxanthin and zeaxanthin, Figs. 2d and 6b, respectively) showed a strong increase under HL conditions. The uncoupling between Chl *a* and the main photosynthetic accessory pigments in response to light change could be a signal of a special photoacclimative strategy developed by this species under low light stress.

Organic Carbon and Nitrogen

Cellular carbon and nitrogen concentrations were significantly correlated ($p<0.001$) and both strongly related to PFD regimes with lower concentrations under high light and vice-versa (Fig. 3a).

The Chl *a* : POC ratio varied slightly, increasing a little from LL to HL regimes (Fig. 3b), mainly due to the decrease of POC along the light gradient.

The POC : PON ratio, ranging between 4.80 ± 0.24 and 6.82 ± 0.08, increased from low to high PFD regime (Fig. 3c) and was significantly correlated to growth rate (r^2 = 0.98, Fig. 3d).

Photosynthetic parameters

The maximal photosynthetic rate ($_{abs}ETR_{max}$) increased from the LL to HL regimes, reaching a maximum at HL1 and then decreasing a little under HL2 (Fig. 4a). A significantly correlated trend between $_{abs}ETR_{max}$ and growth rate was observed (Fig. 4b). Under HL2, Chl *a* enhancement without any related increase in electron transport rate prevented this light condition fitting a linear regression. Indeed, when ETR was not reported in relation to Chl *a* concentration, the relationship between $_{rel}ETR_{max}$ and growth rate was highly significant and linear over all the PFD range (r^2 = 0.92; Fig. 4c).

The photosynthetic efficiency (α^B, Fig. 4d) showed a maximum under the ML condition in agreement with the 100 µmol photons m^{-2} s^{-1} pre-acclimation period of cells, and decreased with higher PFDs. Low values of α^B under low LL1 and LL2 (similar to the HL1 and HL2 ones) might reflect a limited capacity for photosynthetic acclimation at low PFDs. Indeed, the light saturation index (Ek) did not decrease under the value of 200 µmol photons m^{-2} s^{-1}, whereas it increased to almost 1000 µmol photons m^{-2} s^{-1} in agreement with the light-acclimated state of this species (Fig. 4e). The high values of Ek indicated that cells were subjected to limiting or sub-optimal irradiance during light periods in all the five experimental conditions. The amplitude of light limitation, estimated with the Ek : PFD ratio, ranged between 24 and 2 (Fig. 4f), with LL1 and LL2 having values higher than 10.

Photophysiology and the xanthophyll cycle

The PSII maximum photochemical efficiency (Fv : Fm) showed a small range of variation, with the highest value under LL1 (0.61, Fig. 5a) and the lowest under HL1 (0.56, 250 µmol photons m^{-2} s^{-1}). Under HL1 and HL2, *Phaeomonas sp.* developed non-

photochemical quenching (Fig. 5b), while it did not under lower PFD regimes, with the exception of LL1.

A significant linear correlation was found between NPQ and the photoprotective pigment zeaxanthin [Zx : (Vx + Ax + Zx)], suggesting a relevant role of Zx in the development of NPQ in *Phaeomonas sp.* (Fig. 6a). Zx contribution to the xanthophyll cycle was low (less than 10%) revealing the limited need for photoprotection, in relation with the gradual PFD increase and the not so extreme irradiance peak applied during the experimental conditions.

The highest values of Zx were found in cultures grown under HL1 and HL2 (Fig. 6b). The two pigments Vx and Ax, expressed per cell (data not shown), followed the same trend of Chl *a* and other accessory photosynthetic pigments $cell^{-1}$ (see Fig. 2).

Daily evolution of Zx (Fig. 6c) showed that only under the HL2 condition did this pigment increase significantly at midday. Even though NPQ was similar between the two HLs, Zx concentration differed between the two conditions suggesting that a proportion of zeaxanthin was not involved in NPQ development. The morning value of Zx under the HL2 regime was higher than the values measured during each of the HL1 sampling times, revealing a daily-persisting photoprotective state.

DISCUSSION

Chl *a* content in *Phaeomonas sp.* RCC503 (~ 2×10^{-16} mol Chl *a* $cell^{-1}$, cell size ~ 3.3 µm) is in the range of values measured in other small size algal species (Dimier *et al.*, 2007, 2009 b). Combining this study with data from Dimier *et al.* (2009 b), a highly significant correlation between size and Chl *a* $cell^{-1}$ content was obtained (6 species with size ranged between 1.8 and 4.0 µm, $r^2 = 0.92$) proving the direct relevance of size in determining pigment content in small species. Taxonomical difference does not affect the relation between size and Chl *a*, while processes such as photoacclimation have a small effect on this relation in picoeukaryotes (Dimier *et al.*, 2009 b, this study). Indeed, variations in cell size are so small over the irradiance range that any allometric effect (see Finkel *et al.*, 2010) becomes undetectable.

Physiological response curves show that *Phaeomonas sp.* RCC503 grows properly under a broad range of PFD (from 100 to 500 µmol photons m^{-2} s^{-1}), meaning it was able to

adequately cope with different light environments thanks to efficient photoacclimative processes concerning both cell physiology and biochemistry. This is consistent with its origin from a Mediterranean coastal area, i.e. adapted to grow under variable light conditions.

Increase in Chl c_3 under low light has been found in many species both in laboratory (Rodriguez *et al*., 2006; Dimier *et al*., 2009 a) and in field experiments, where higher Chl c_3 values were found in the Deep-Chlorophyll Maximum layer (Brunet *et al*., 2007), in agreement with its efficient role in light harvesting (Johnsen and Sakshaug, 1993). Thus, our study reinforces the hypothesis of a photoacclimative role of this pigment and demonstrates that changes in Chl c_3 are independent of other pigments, such as fucoxanthin, Chl c_2 and Chl *a*. Since Chl c_3 is broadly present in phytoplankton species, and in many picoeukaryotes, this result would need further investigation to understand the ecological advantage in synthesizing such a pigment and how its synthetic pathway would work.

The significant relation between photosynthetic rate, cell biochemistry changes and growth rate suggests a direct and functional link between PFD, photoacclimation, photosynthetic and growth rate. In many studies, the variability of the relationship between photosynthetic organic matter production and cell growth has been highlighted (Litchman, 2000), growth and photosynthetic parameters being poorly coupled (van Leeuwe *et al*., 2005). This variability has been attributed to factors such as variations in respiration rates, dissolved organic matter loss from cells, and changed extent of metabolites storage such as polysaccharides (van Leeuwe *et al*., 2005).

The observed result is probably linked to the experimental conditions we applied. Simulating what occurs in nature, the sinusoidal irradiance evolution causes cells to experience a low or moderate daily-integrated PFD with a short irradiance peak. Our experimental conditions prevented either continuous high light or continuous limited light stress as occurs under quadratic light evolution. Small cell size limits the intracellular storage of energy (Raven, 1998) that might enhance the coupling of photosynthesis and growth rate, as already discussed by Dimier *et al*. (2009 a) for the picoeukaryote *Pelagomonas calceolata*.

Growth rate is linearly related to both Ek : PFD ($r^2 = 0.96$, $p<0.001$) and the POC : PON ratio ($r^2 = 0.98$, $p<0.001$), these two ratios being correlated ($r^2 = 0.95$, $p<0.001$). These results indicate a functional and linear link between PFD and growth rate through photosynthetic rate adjustments and consequently changes in cellular biochemistry. The great range of variation of the POC : PON ratio (35%, between 4.80 to 6.50) reveals significant biochemical modifications related to irradiance and growth rate variations (e.g., Finkel *et al*., 2010).

Higher values of POC : PON obtained under the higher PFD conditions are close to the Redfield ratio, a result that led us to reinforce the hypothesis of an optimal physiological state of cells under high light.

Growth rate being the highest under HL2 condition, the photoacclimative strategy adopted by *Phaeomonas sp.* is efficient. This species belongs to the "light adapted" functional category (Falkowski and Owens, 1980; Falkowski, 1983), as also suggested by the high light saturation for photosynthesis (Ek) estimated from the ETR-light curves. Under the HL2 condition, the small decrease of maximal photosynthetic rate per Chl *a* unit ($_{abs}ETR_{max}$) compared to the HL1 condition while growth rate still increased relatively could be due to the Chl *a* $cell^{-1}$ increase. Indeed, the relation between $_{rel}ETR_{max}$ and growth rate is linear over the light gradient (Fig. 4c). Increase in both Chl *a* and accessory photosynthetic pigments under the HL2 condition suggests the development of a σ-type photoacclimation strategy aiming to increase the size of light harvesting antennae (Six *et al*., 2008, Dimier *et al*., 2009 a). Increase in photosynthetic pigments under the highest PFD condition was surprising since cells developed photoprotection when irradiance reached its maximum. Comparison with HL1 condition, where no pigment increase was noticeable, pigment enhancement under HL2 condition might be related to the strongest photoprotection. Both the higher level of Zx and its persistent presence in cells growing under the HL2 condition (even before the irradiance peak) indicate a photoprotective state of PSII.

The photoprotective state of HL2 and HL1 cells would also lead to a decreased photosynthetic efficiency, which is demonstrated by the decrease of α^B. Since the gradual PFD increase, cells quickly perform photophysiological regulation processes explaining both the low value of DPS (<15%) and its efficiency in protecting PSII (see Dimier *et al*.,

2009 a). The highest NPQ value has been reached already under HL1 and no further increase can be observed under HL2 probably in relation to the development of other photoprotective mechanisms such as PSII conformational changes. Additional molecules of Zx under HL2 condition do not have a direct role in NPQ functioning. It is known that Zx molecules are able to indirectly protect PSII through changes in thylakoidal membrane fluidity, or preventing lipid peroxidation (see Goss and Jakob, *in press*). The neoxanthin trend is similar to the one of Zx either over the irradiance range (Fig. 2d) or over the day under HL2 (data not shown). This feature might be related to a role of Neox in preserving PSII from photo-inactivation and protecting membrane lipids as recently demonstrated in plants (Dall'Osto *et al*., 2007).

This photoprotective status found in cells grown under HL2 might be explained by the rapid kinetics of PFD increase, also linked to the higher irradiance reached, or also by the increase in accessory photosynthetic pigments, which might have enhanced the sensitivity of PSII to high light. The role of photoprotective pigments as a trap for a part of the harvested electrons would thus decrease the quantum yield leading to an energy-deficient state during low light periods that would in turn require an increase in the light-harvesting pigment content. This last hypothesis supposes a feedback-relationship between photoprotection and photoacclimation aiming to enhance the light harvesting capacity of cells. Cells would perceive both high light values and low light dose per day (e.g., through the time spent under low light) and respond to both these factors. Such a special physiological plasticity is likely to ocurr in species growing in coastal waters where high vertical mixing implies fast shifts between high and low light conditions. This hypothesis agrees with the results obtained by Dimier and co-workers (2009 b) where it has been shown that coastal species are physiologically "intermediary" compared to surface-offshore and deep water species, in terms of both photosynthetic and photoprotective pigment content. Further studies are needed to test this hypothesis and to obtain clearer knowledge on the ecophysiological capacity of coastal phytoplankton, such as many diatoms, to efficiently photoacclimate and photoprotect.

Phaeomonas sp. is not able to grow under strong light limitation (e.g., for a Ek : PFD ratio > 10). The fact that the increase in Chl *a* is not coupled with an increase in photosynthetic accessory pigments might suggest an enhancement in number of PSII

reaction centers more than in the size of the light-harvesting complexes, distinctive of a n-type photoacclimation strategy (Six *et al*., 2008). The heavy nutrient cost for low-light growth required by the n-type photoacclimation strategy and its higher-energy cost (Six *et al.*, 2008) can limit or inhibit growth (Dimier *et al*., 2009 b).

The same photoacclimation strategy has been observed in other picoeukaryotes, the lagoon ecotype of *Ostreococcus tauri* (Six *et al*., 2008) and the low-light–adapted *Pelagomonas calceolata* (Dimier *et al*., 2009 a). The latter (Dimier *et al*., 2009 a) as well as the present study have shown how some species can develop either the *σ*- or n-type photoacclimation strategy in relation to the light conditions experienced. The *n*-type photoacclimation strategy would evolve when daily the PFD dose is very low or when cells spend a long time under low light in order to increase their photochemistry (Dimier *et al*., 2009 a). This result differs from what was shown by Six *et al*. (2008) in two *Ostreococcus* ecotypes (Six *et al*., 2008), where the n-type photoacclimation evolved in the lagoon ecotype with decreasing growth irradiance. The inconsistency between these studies could be related to the differences of experimental design, since the present study (as Dimier *et al.*, 2009 a) applied a sinusoidal irradiance regime, while the work done by Six *et al.* (2008) employed a continuous irradiance over the light period. Supporting such a hypothesis, Dimier *et al*. (2009 a) showed that the main factor responsible for developing the n- or *σ*-type photoacclimation was the frequency of irradiance variation during the daylight period.

The very low-light condition surprisingly induces both NPQ generation and little increase in Zx and Neox. Zx and NPQ formation reveals the development of a trans-thylakoidal proton gradient probably caused by chlororespiration (Goss and Jakob, *in press*, and references therein) or by a putative water-water cycle (Mehler's reaction, Badger *et al*., 2000). It is noteworthy that Neox has a role against photooxidation and would be particularly active when Mehler's reaction takes place (Dall'Osto *et al*., 2007).

ACKNOWLEDGEMENTS

The authors gratefully acknowledge Ferdinando Tramontano for his help during experiments and HPLC analysis. Enzo Saggiomo and Francesca Margiotta are acknowledged for using the spectrophotometer and the CHN and for sharing the PAM

probe. Vasco Giovagnetti acknowledges the SZN for his PhD grant. We would like to thank Dr. D. Campbell and the other anonymous referee for their comments and helping suggestions improving the quality of the manuscript.

REFERENCES

Badger, M.R., Caemmerer, von, S., Ruuska, S. and Nakano, H. (2000) Electron flow to oxygen in higher plants and algae: rates and control of direct photoreduction (Mehler reaction) and rubisco oxygenase. *Phil. Trans. R. Soc. Lond. B*, **355**, 1433-1446.

Brunet, C., Casotti, R., Vantrepotte, V., Corato, F. and Conversano, F. (2007) Vertical variability and diel dynamics of picophytoplankton in the Strait of Sicily (Mediterranean Sea) in summer. *Mar. Ecol. Prog. Ser.*, **346**, 15-26.

Dall'Osto, L., Cazzaniga, S., North, H., Marion-Poll, A. and Bassi, R. (2007) The *Arabidposis aba4-1* mutant reveals a specific function for neoxanthin in protection against photooxidative stress. *The Plant Cell*, **19**, 1048-1064.

Dimier, C., Saviello, G., Tramontano, F. and Brunet, C. (2009b) Comparative ecophysiology of the xanthophyll cycle in six marine phytoplanktonic species. *Protist*, **160**, 397-411.

Dimier, C., Brunet, C., Geider, R. and Raven, J.A. (2009a) Growth and photoregulation dynamics of the picoeukaryote *Pelagomonas calceolata* in fluctuating light. *Limnol. Oceanogr.*, **54**, 823-836.

Dimier, C., Corato, F., Tramontano, F. and Brunet, C. (2007b) Photoprotection and xanthophyll cycle activity in three diatoms. *J. Phycol.*, **43**, 937-947.

Dimier, C., Corato, F., Saviello, G. and Brunet, C. (2007a) Photo-physiological properties of the marine picoeukaryote *Picochlorum RCC237* (Trebouxiophyceae, Chlorophyta). *J. Phyco.l*, **43**, 275-283.

Eilers, P.H.C. and Peeters, J.C.H. (1988) A model for the relationship between light intensity and the rate of photosynthesis in phytoplankton. *Ecol. Model.* **42**, 199-215.

Falkowski, P. (1983) Light-shade adaptation and vertical mixing of marine phytoplankton: a comparative field study. *J. Mar. Res.*, **41**, 215-237.

Falkowski, P. and Owens, T.G. (1980) Light-shade adaptation: two strategies in marine phytoplankton. *Plant Physiol.*, **66**, 592-595.

Finazzi, G., Johnson, G. N., Dall'osto, L., Zito, F., Bonente, G., Bassi, R. and Wollman, F. A. (2006) Non-photochemical quenching of chlorophyll fluorescence in *Chlamydomonas reinhardtii*. *Biochemistry*, **45**, 1490–1498.

Finkel, Z., Beardall, J., Flynn, K. J., Quigg, A., Rees, T. A. and Raven, J. A. (2010) Phytoplankton in a changing world: cell size and elemental stoichiometry. *J. Plankton Res.*, **32**, 119-137.

Hedges, J.I. and Stern, J.H. (1984) Carbon and nitrogen determination of carbonate-containing solids. *Limnol. Oceanogr.*, **29**, 657-663.

Goss, R. and Jakob, T. (2010) Regulation and mechanism of xanthophyll cycle-dependent photoprotection in algae. *Photosynthesis Res*, in press.

Guillard, R. R. and Ryther, J.H. (1962) Studies of marine planktonic diatoms. I. *Cyclotella nana* Hustedt and *Detonula confervacea* (Cleve) Gran. *Can. J. Microbiol.*, **8**, 229-38.

Johnsen, G., Sakshaug, E. (1993). Bio-optical characteristics and photoadaptive responses in the toxic and bloomforming dinoflagellates *Gyrodinium aureolum*, *Gymnodinium galatheanum*, and two strains of *Prorocentrum minimum*. *J. Phycol.*, **29**, 627-642.

Lavaud, J., Strzepeck, R. F. and Kroth, P.G. (2007) Photoprotection capacity differs among diatoms: possible consequences on the spatial distribution of diatoms related to fluctuations in the underwater light climate. *Limnol. Oceanogr.*, **52**, 1188-1194.

Lewis, M. R., Horne, E. P. W., Cullen, J. J., Oakey, N. S. and Platt T. (1984) Turbulent motions may control phytoplankton photosynthesis in the upper ocean. *Nature* **311:** 49–50.

Litchman, E. (2000) Growth rate of phytoplankton under fluctuating light. *Freshw. Biol.*, **44**, 223-235.

Litchman, E. and Klausmeier, C. A. (2001) Competition of phytoplankton under fluctuating light. *Am. Nat.*, **157**, 170–87.

MacIntyre, H. L., Kana T. M., and Geider R. J. (2000) The effect of water motion on short-term rates of photosynthesis by marine phytoplankton. *Trends Plant Sci.*, **5**, 12–17.

MacIntyre, H. L., Kana T. M., Anning T. and Geider R. J. (2002) Photoacclimation of photosynthesis irradiance response curves and photosynthetic pigments in microalgae and cyanobacteria. *J. Phycol.*, **38**, 17–38.

Not, F., Massana, R., Latasa, M., Marie, D., Colson, C., Eikrem, W., Pedrós-Alió, C., Vaulot, D. and Simon, N. (2005) Late summer community composition and abundance of photosynthetic picoeukaryotes in Norwegian and Barents Sea. *Limnol. Oceanogr.*, **50**, 1677–86.

Peek, M. S., Russek, E., Wait, C. D. A. and Forseth I. N. (2002) Physiological response curve analysis using nonlinear mixed models. *Oecologia*, **132**, 175-180.

Rascher, U. and Nedbal, L. (2006) Dynamics of photosynthesis in fluctuating light. *Curr. Opin. Plant. Biol.*, **9**, 671-678.

Raven, J. A. (1998) The twelfth Tansley lecture. Small is beautiful: the picophytoplankton. *Funct. Ecol.*, **12**, 503.

Raven, J. A., Finkel, Z. V. and Irwin A. J. (2005) Picophytoplankton: Bottom-up and top-down controls on ecology and evolution. *Vie Milieu*, **55**, 209–215.

Raven, J. A., and Geider R. (2003) Adaptation, acclimation, and regulation in algal photosynthesis. *In* S. E. D. A. W. Larkum, and J. A. Raven [ed.], Advances in photosynthesis and respiration Vol 14, Photosynthesis in Algae. *Advances in Photosynthesis. Kluwer Academic Publishers*.

Rodriguez, F., Chauton, M., Johnsen, G., Andresen, K., Olsen, L. M. and Zapata, M. (2006) Photoacclimation in phytoplankton: implications for biomass estimates, pigment functionality and chemotaxonomy. *Mar. Biol.*, **148**, 963-971.

Six, C., Finkel, Z., Rodriguez, F., Marie, D., Partensky, F. and Campbell D. A. (2008) Contrasting photoacclimation costs in ecotypes of the marine eukaryote picoplankter *Ostreococcus*. *Limnol. Oceanogr.*, **53**, 255-265.

Six C., Sherrard, R., Lionard M., Roy S., Campbell D.A. (2009) Photosystem II and pigment dynamics among ecotypes of the Green Alga *Ostreococcus*. *Plant Physiol*.,**151**, 379-390.

Stransky, H., Hager, A. (1970) Das Carotinoidmuster und die verbreitung des lichtinduzierten Xanthophyllcyclus in verschiedenen Algenklassen. II. Xanthophyceae. *Arch. Mikrobiol*., **71**, 164-190.

Timmermans, K. R., van der Wagt, B., Veldhuis, M. J. W., Maatman, A. and de Baar, H. J. W. (2005) Physiological responses of three species of marine pico-phytoplankton to ammonium, phosphate, iron and light limitation. *J. Sea Res.*, **53**,109–120.

Worden, A. Z. and Not, F. (2008) Ecology and diversity of picoeukaryotes. *Microbial Ecology of the Oceans, Second Edition*, 159-205.

Van Leeuwe, M. A., Sikkelerus, van B., Gieskes W. W. C. and Stefels, J. (2005) Taxon-specific differences in photoacclimation to fluctuating irradiance in an Antarctic diatom and a green flagellate. *Mar. Ecol. Prog. Ser.*, **288**, 9-19.

Vaulot, D., Le Gall, F., Marie, D., Guillou, L. and Partensky, F. (2004) The Roscoff Culture Collection (RCC): a collection dedicated to marine picoplankton. *Nova. Hedwigia* **79**, 49-70.

FIGURE LEGENDS

Fig. 1. (**a**) The five sinusoidal light regimes applied during the study, with different maximal PFD peaks (10, 50, 100, 250 and 500 µmol photons m^{-2} s^{-1}, respectively). Arrows indicate sampling. (**b**) Evolution of growth rate of *Phaeomonas sp.* over the light conditions. Data are the average of three measurements per three days (corresponding to the exponential growth phase for HL and ML conditions), error bars are SD.

Fig. 2. Evolution of: chlorophyll *a* $cell^{-1}$ expressed in 10^{-16} mol Chl *a* $cell^{-1}$ (**a**), chlorophyll c_2 $cell^{-1}$ (white dots) and chlorophyll c_3 $cell^{-1}$ (black dots) expressed in 10^{-16} mol pigment $cell^{-1}$ (**b**), fucoxanthin $cell^{-1}$ (white squares), *cis*-fucoxanthin $cell^{-1}$ (white triangles) and β-carotene $cell^{-1}$ (grey dots) expressed in 10^{-16} mol pigment $cell^{-1}$ (**c**), and neoxanthin $cell^{-1}$ content in 10^{-17} mol pigment $cell^{-1}$ (**d**), over the five PFD conditions. Chl *a*, chlorophyll *a*; Chl c_2, chlorophyll c_2; Fuco, fucoxanthin; *cis*-Fuco, *cis*-fucoxanthin; β-Car, β-carotene, Neox, neoxanthin. Data are the average of three measurements per three days (corresponding to the exponential growth phase for HL and ML conditions), error bars are SD.

Fig. 3. Evolution of: cellular organic carbon (POC, white squares) and nitrogen (PON, black squares) concentrations (pg $cell^{-1}$) (**a**), Chl *a* : POC ratio expressed in 10^{-18} mol Chl a^{-1} pg C^{-1} (**b**), and POC : PON ratio (**c**), over the five PFD conditions. Relationship between POC : PON ratio and growth rate (r^2 = 98) (**d**). Data are the average of three measurements per three days (corresponding to the exponential growth phase for HL and ML conditions), error bars are SD.

Fig. 4. (**a**) Evolution of the maximal photosynthetic rate ${}_{abs}ETR_{max}$ (in mol e^- g Chl a^{-1} h^{-1}) over the five PFD conditions. Relationship between growth rate and ${}_{abs}ETR_{max}$ (**b**) or ${}_{rel}ETR_{max}$ (**c**). Evolution of α^B (mol e^- g Chl a^{-1} h^{-1} [µmol photons m^{-2} s^{-1}]$^{-1}$, **d**), Ek (in

µmol photons m^{-2} s^{-1}, **e**) and Ek : PFD ratio (**f**) over the five PFD conditions. Data are the average of three measurements per three days (corresponding to the exponential growth phase for HL and ML conditions), error bars are SD.

Fig. 5. Evolution of the maximal photochemical efficiency (Fv : Fm; **a**) and non-photochemical quenching (NPQ; **b**) over the five PFD conditions. Data are the average of three measurements per three days (corresponding to the exponential growth phase for HL and ML conditions), error bars are SD.

Fig. 6. (**a**) Relationship between Zx : (Vx + Ax + Zx) and NPQ (non-photochemical quenching). (**b**) Evolution of zeaxanthin Chl a^{-1} (Zx Chl a^{-1} in 10^{-2} mol : mol Chl *a*) over the five PFD conditions. (**c**) Mean of zeaxanthin $cell^{-1}$ in the three samples of the dawn, irradiance peak and sunset under the HL1 and HL2 regimes. Data are the average of three measurements per three days (corresponding to the exponential growth phase for HL and ML conditions), error bars are SD.

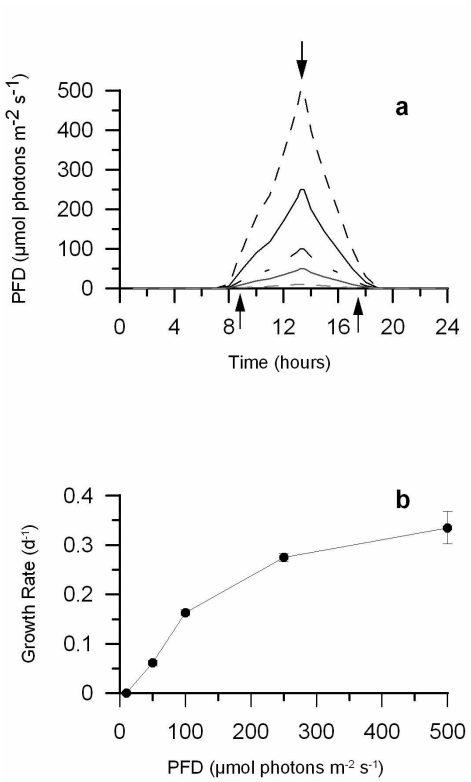

Giovagnetti et al._Fig. 1

89x231mm (300 x 300 DPI)

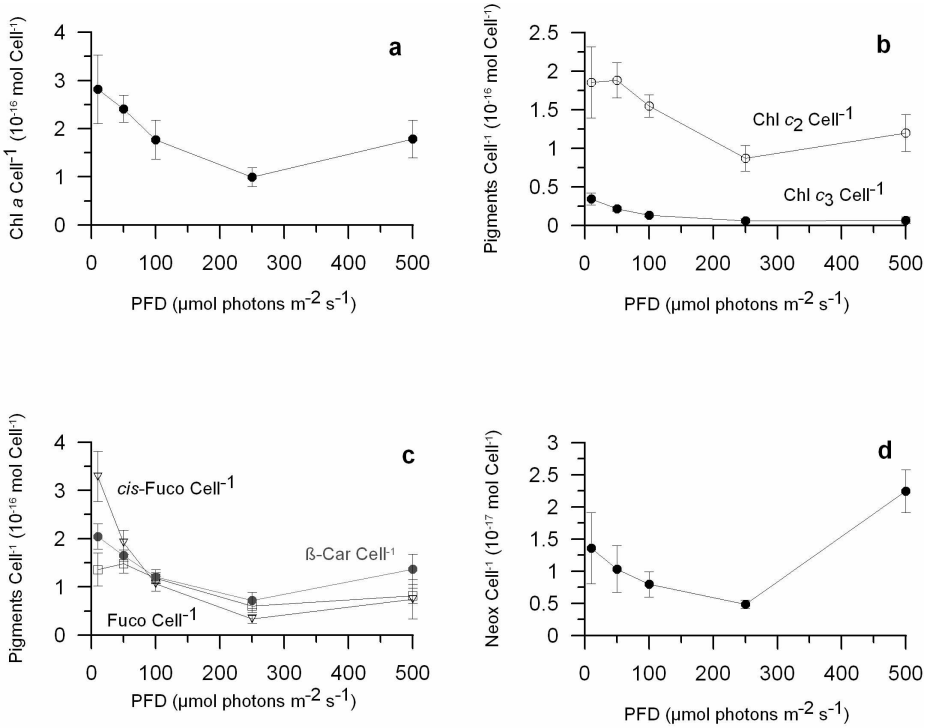

Giovagnetti et al._Fig. 2

182x236mm (300 x 300 DPI)

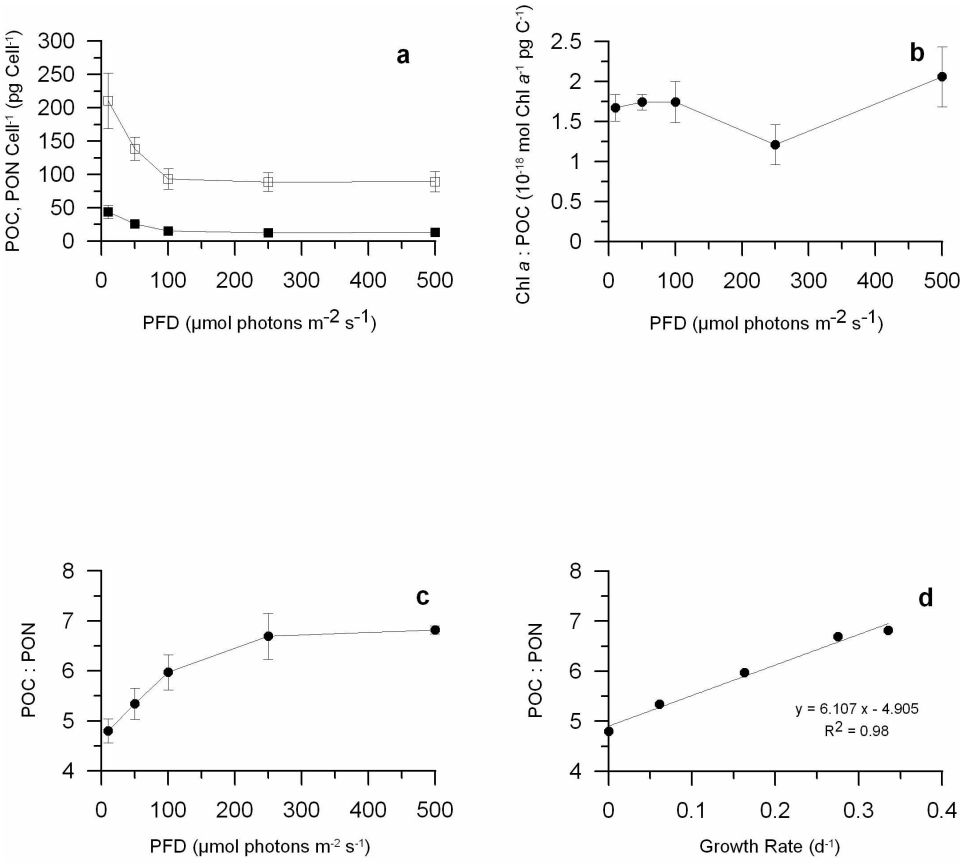

Giovagnetti et al._Fig. 3

182x228mm (300 x 300 DPI)

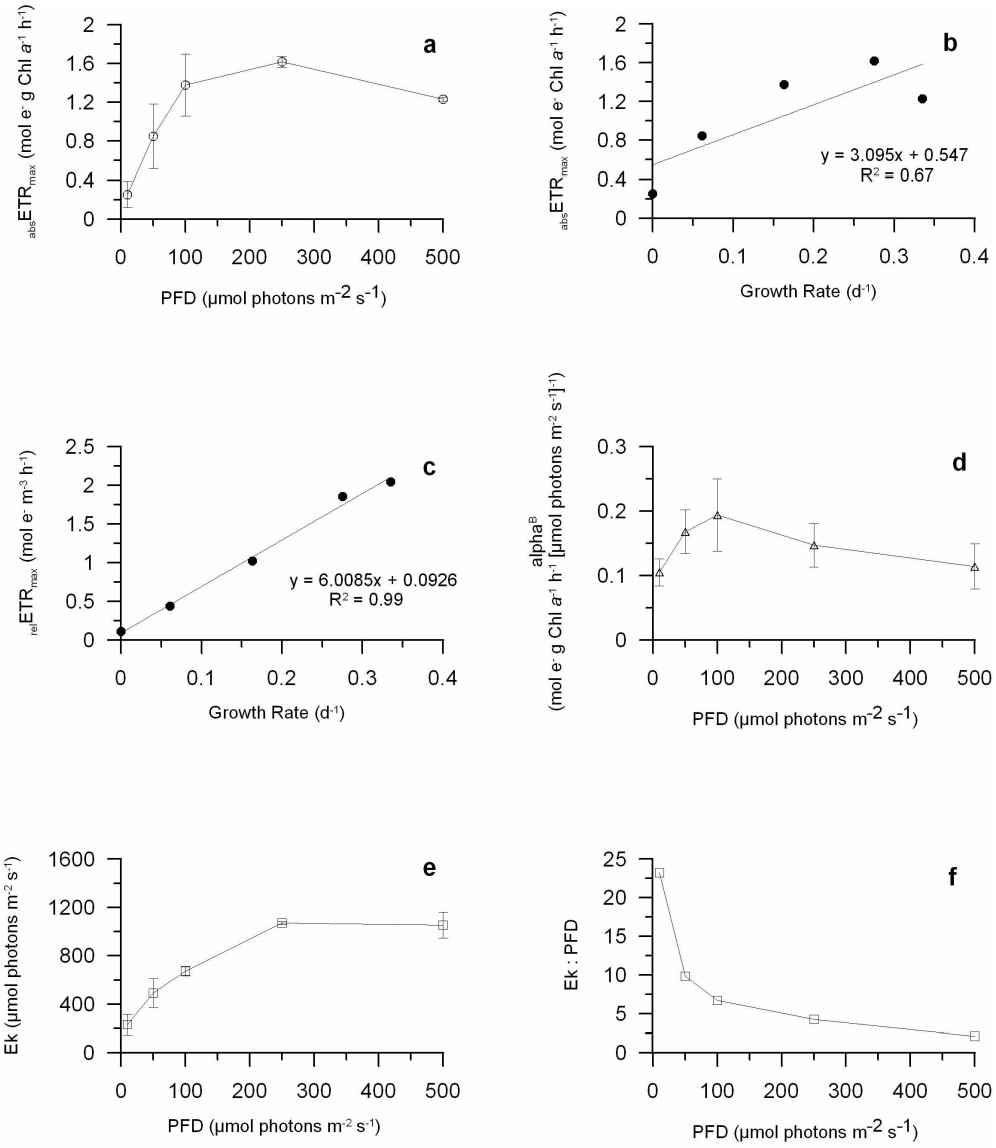

Giovagnetti et al._Fig. 4

195x236mm (300 x 300 DPI)

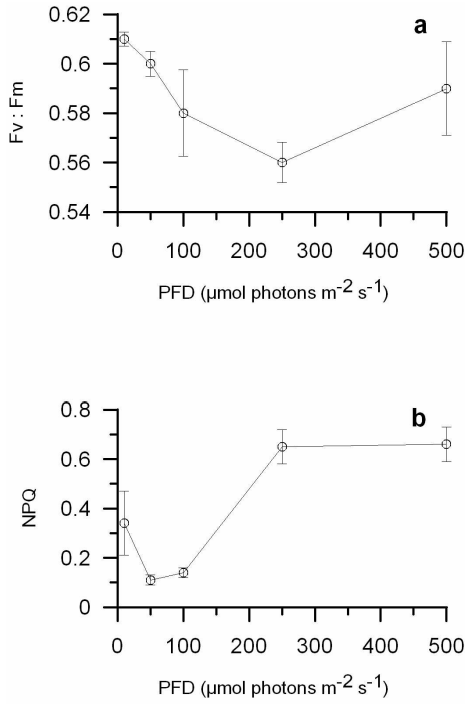

Giovagnetti et al._Fig. 5

88x231mm (300 x 300 DPI)

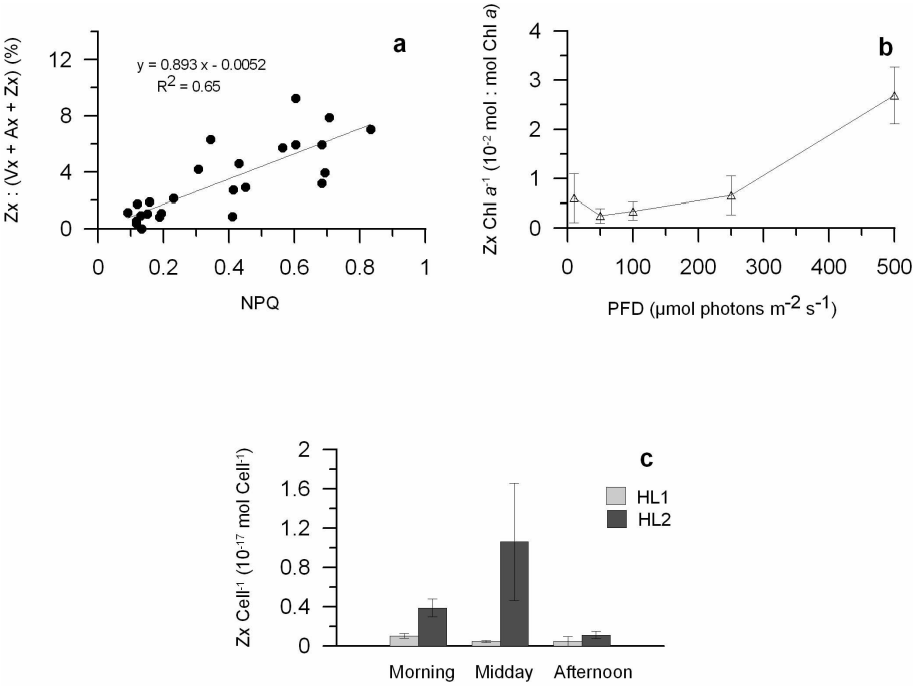

Giovagnetti et al._Fig. 6

176x232mm (300 x 300 DPI)